

Role of Multidetector Ct in Characterization of Renal Mass

Zahraa Muhammad Hassan Marhoon ¹, Sahla Baqir Zain Al-Abidin Abbas ², Taiba Safaa Anwar Sobhi ³

¹Al-Mustaqbal University
College - Applied Medical
Physics, Iraq

²Al-Mustaqbal University
College - Applied Medical
Physics, Iraq

³Al-Mustaqbal University
College - Applied Medical
Physics, Iraq

Background: Due to rapid pace in development of imaging techniques and increasing number of investigations being done, more number of renal masses are discovered incidentally during evaluation of unrelated or unspecific symptoms. Hence it is vital to differentiate neoplastic and non-neoplastic masses.

Among the neoplastic masses, there is a need to differentiate benign and malignant masses so that appropriate treatment strategies like nephron sparing surgery, radio frequency ablation etc. can be planned at an early stage and avoiding unnecessary radical treatments for improved patients survival.

Methods: many non-consecutive patients belonging to all ages and both sexes admitted into the various clinical departments of Hilla General Teaching Hospital who had presented with suspected renal mass by clinical signs and symptoms were examined on CT with protocol were included in our study. **Results:** CT is the standard imaging modality of choice for characterization and staging of the renal lesions.

Conclusions: Computed Tomography (Multidetector) is the imaging modality of choice for further evaluation and characterization. Contrast enhanced CT is done in four phases viz., unenhanced, corticomedullary, nephrographic and excretory phase especially in cases of malignancy like renal cell carcinoma and benign conditions like angiomyolipoma and abscess is sufficient. However histopathological is the gold standard for diagnosis of various renal masses.

Keywords: Computed tomography, renal masses.

Corresponding Author: Zahraa Muhammad Hassan Marhoon †, Al-Mustaqbal University College - Applied Medical Physics, Iraq

Copyright : © 2024 The Authors. Published by Publisher. This is an open access article under the CC BY-NC-ND license (<https://creativecommons.org/licenses/by-nc-nd/4.0/>).

Supplementary information The online version of this article (<https://doi.org/xx.xxx/xxx.xx>) contains supplementary material, which is available to autho-rized users.

Introduction

Historical introduction

A CT scan or computed tomography scan (formerly known as computed axial tomography or CAT scan) is a medical imaging technique used in radiology (x-ray) to obtain detailed internal images of the body noninvasively for diagnostic purposes. The personnel that perform CT scans are called radiographers or radiology technologists.

1.2.Modern CT scanner



CT scanners use a rotating X-ray tube and a row of detectors placed in the gantry to measure X-ray attenuations by different tissues inside the body. The multiple X-ray measurements taken from different angles are then processed on a computer using reconstruction algorithms to produce tomographic (cross-sectional) images (virtual "slices") of a body. The use of ionizing radiation sometimes restricts its use owing to its adverse effects. However, CT can be used in patients with metallic implants or pacemakers, for whom MRI is contraindicated.

Since its development in the 1970s, CT has proven to be a versatile imaging technique. While CT is most prominently used in diagnostic medicine, it also may be used to form images of non-living objects. The 1979 Nobel Prize in Physiology or Medicine was awarded jointly to South African-American physicist Allan M. Cormack and British electrical engineer Godfrey N. Hounsfield "for the development of computer-assisted tomography". The first commercially viable CT scanner was invented by Sir Godfrey Hounsfield in Hayes, United Kingdom, at EMI Central Research Laboratories using X-rays. Hounsfield conceived his idea in 1967.[4] The first EMI-Scanner was installed in Atkinson Morley Hospital in Wimbledon, England, and the first patient brain-scan was done on 1 October 1971.[18] It was publicly announced in 1972.

The original 1971 prototype took 160 parallel readings through 180 angles, each 1° apart, with each scan taking a little over 5 minutes. The images from these scans took 2.5 hours to be processed by algebraic reconstruction techniques on a large computer. The scanner had a single photomultiplier detector, and operated on the Translate/Rotate principle.[18]

It is often claimed that revenues from the sales of The Beatles records in the 1960s helped fund the development of the first CT scanner at EMI[19] although this has recently been disputed.[20] The first production X-ray CT machine (in fact called the "EMI-Scanner") was limited to making tomographic

sections of the brain, but acquired the image data in about 4 minutes (scanning two adjacent slices), and the computation time (using a Data General Nova minicomputer) was about 7 minutes per picture. This scanner required the use of a water-filled Perspex tank with a pre-shaped rubber "head-cap" at the front, which enclosed the patient's head. The water-tank was used to reduce the dynamic range of the radiation reaching the detectors (between scanning outside the head compared with scanning through the bone of the skull). The images were relatively low resolution, being composed of a matrix of only 80×80 pixels.

In the U.S., the first installation was at the Mayo Clinic. As a tribute to the impact of this system on medical imaging the Mayo Clinic has an EMI scanner on display in the Radiology Department. Allan McLeod Cormack of Tufts University in Massachusetts independently invented a similar process, and both Hounsfield and Cormack shared the 1979 Nobel Prize in Medicine.

1.3. The physics of computed tomography scan (CT-scan)

The tissues and materials generally differ in their ability to absorb X-rays, where some substances are more permeable to X-rays while some others impermeable and therefore the different tissues seem different when the X-ray film is developed. For example, the dense tissues such as the bones appear white on a CT film while the soft tissues such as the brain or kidney appear gray while the cavities filled with air such as the lungs appear black.

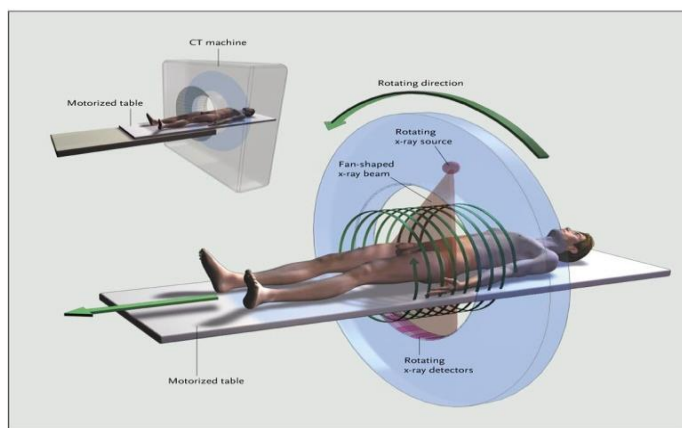


Figure 1 The physics of computed tomography scan (CT-scan) (A)

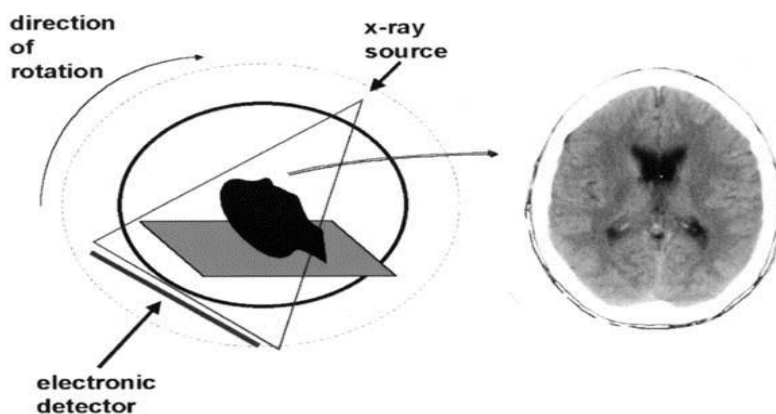


Figure 2 The physics of computed tomography scan (CT-scan) (B)

CT image is composed of a Matrix, each matrix composed of pixels (picture elements) and voxel (volume element) that represents a measurement of the average x-ray attenuation of a box-like extending through the thickness of the tissue section. In addition, in a real CT image, all tissues within a single pixel would be the

same shade of gray .The image can be stored for retrieval and use later. The image can be stored for retrieval and use later.

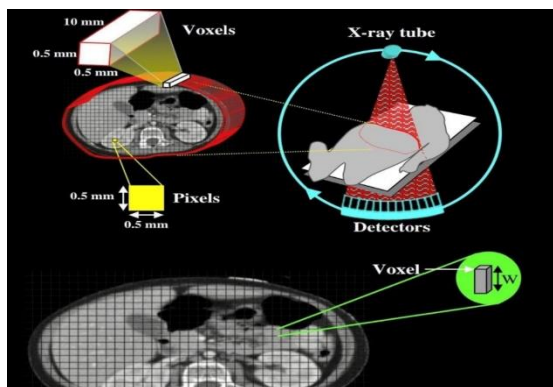


Figure 4The physics of computed tomography scan (CT-scan) (C)

Matrix: Two dimensional grid of pixels, used to compose images on a display monitor. The matrix determines the number of rows and columns

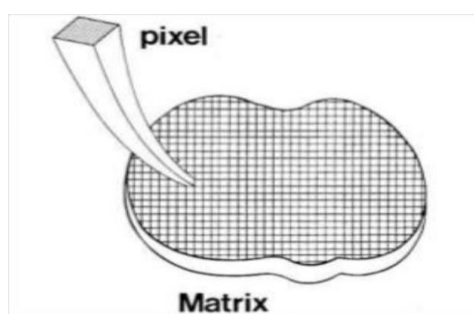


Figure 5The physics of computed tomography scan (CT-scan) (D)

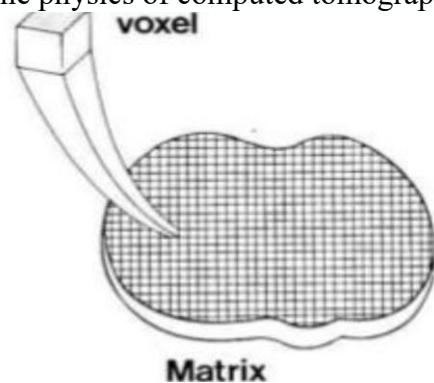


Figure 6 the physics of computed tomography scan (CT-scan) (E)

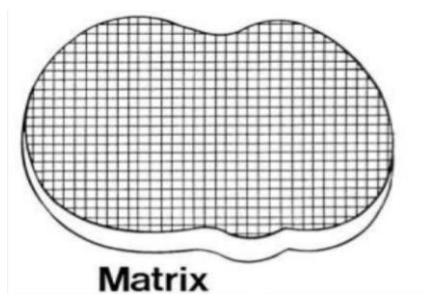
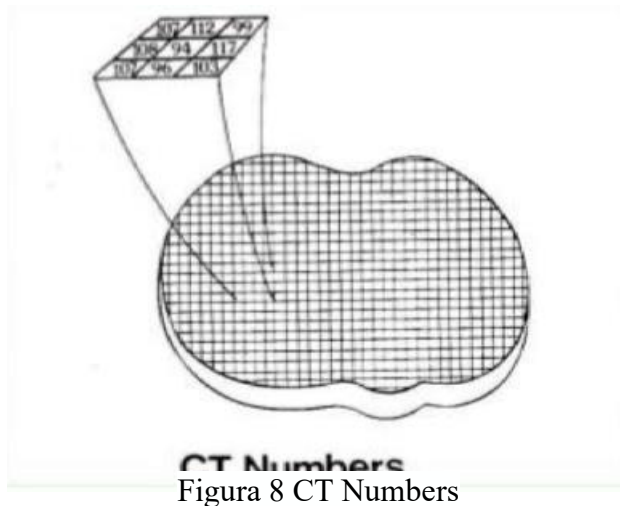


Figure 7The physics of computed tomography scan (CT-scan) (F)



Pixel: Two dimensional picture element that makes up the matrix. Each pixel represents a CT number and is the building block of the matrix and image.

Voxel: Three dimensional element of anatomy represented by the two dimensional Voxel volume = pixel height x pixel width x slice thickness pixel.

Hounsfield Units for human body

<i>Bone</i>	<i>1000</i>
<i>Liver</i>	<i>40 to 60</i>
<i>White Matter</i>	<i>46</i>
<i>Grey Matter</i>	<i>43</i>
<i>Blood</i>	<i>40</i>
<i>Muscle</i>	<i>10 to 40</i>
<i>Kidney</i>	<i>30</i>
<i>Cerebrospinal Fluid</i>	<i>15</i>
<i>Water</i>	<i>0</i>
<i>Fat</i>	<i>-50 to -100</i>
<i>Air</i>	<i>-1000</i>

1.4. CT Numbers

The numbers in the image matrix are called CT numbers. Each pixel has a number which represents the x ray attenuation in the corresponding voxel of the object.

Theoretical Part

This chapter includes a general description of the theoretical part containing the general information about (CT) as well included positioning of the patient, general guidelines and renal pathology.

2.2. Positioning of the Patient

Computed tomography of abdomen (kidneys, ureters and bladder) is best performed with the patient in lie on a narrow table that slides into the center of the CT scanner. Most often, you will lie on your back with your arms raised above your head.

Once you are inside the scanner, the machine's Xray beam rotates around you. Modern spiral scanners can perform the exam without stopping.

A computer creates separate images of the belly area. These are called slices. These images can be stored, viewed on a monitor, or printed on film. Three-dimensional models of the belly area can be made by stacking the slices together.

You must be still during the exam, because movement causes blurred images. You may be told to hold your breath for short periods of time.

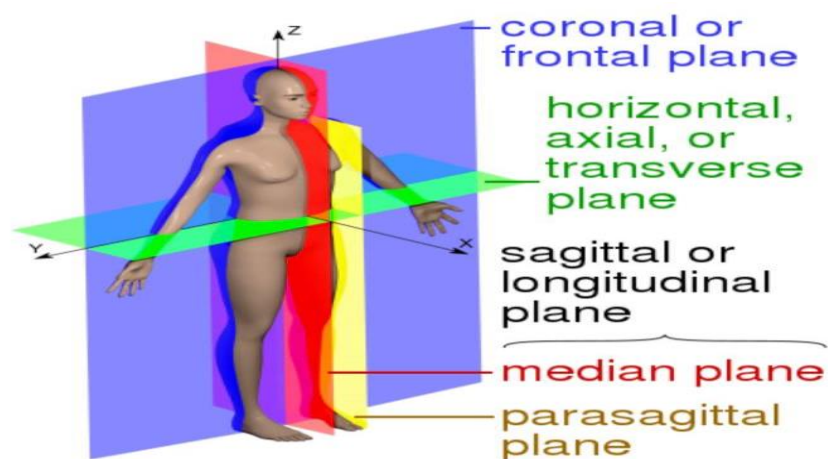
In many cases, an abdominal CT is done .

The scan should take less than 30 minutes.

some institutions may perform a limited pelvic scan in prone if the supine scan shows a calculus near the vesicoureteric junction

stone composition assessment can be done with dual energy CT Findings

- identification of calcified renal tract calculi size and position
- assessment of the sequelae of calculi
- obstruction
- infection
- assessment of other causes of flank pain if negative for calculus disease
- presence of further calculi at risk of obstructing



Anatomical planes in a human:

-  median or sagittal plane
-  a parasagittal plane
-  frontal or coronal plane
-  transverse or axial plane

2.3. Anatomical planes

is a hypothetical plane used to transect the body, in order to describe the location of structures or the direction of movements. In human and animal anatomy, three principal planes are used:

- The sagittal plane or lateral plane (longitudinal, anteroposterior) is a plane parallel to the sagittal suture. It divides the body into left and right.
- The coronal plane or frontal plane (vertical) divides the body into dorsal and ventral (back and front, or posterior and anterior) portions.
- The transverse plane or axial plane (horizontal) divides the body into cranial and caudal (head and tail) portions.

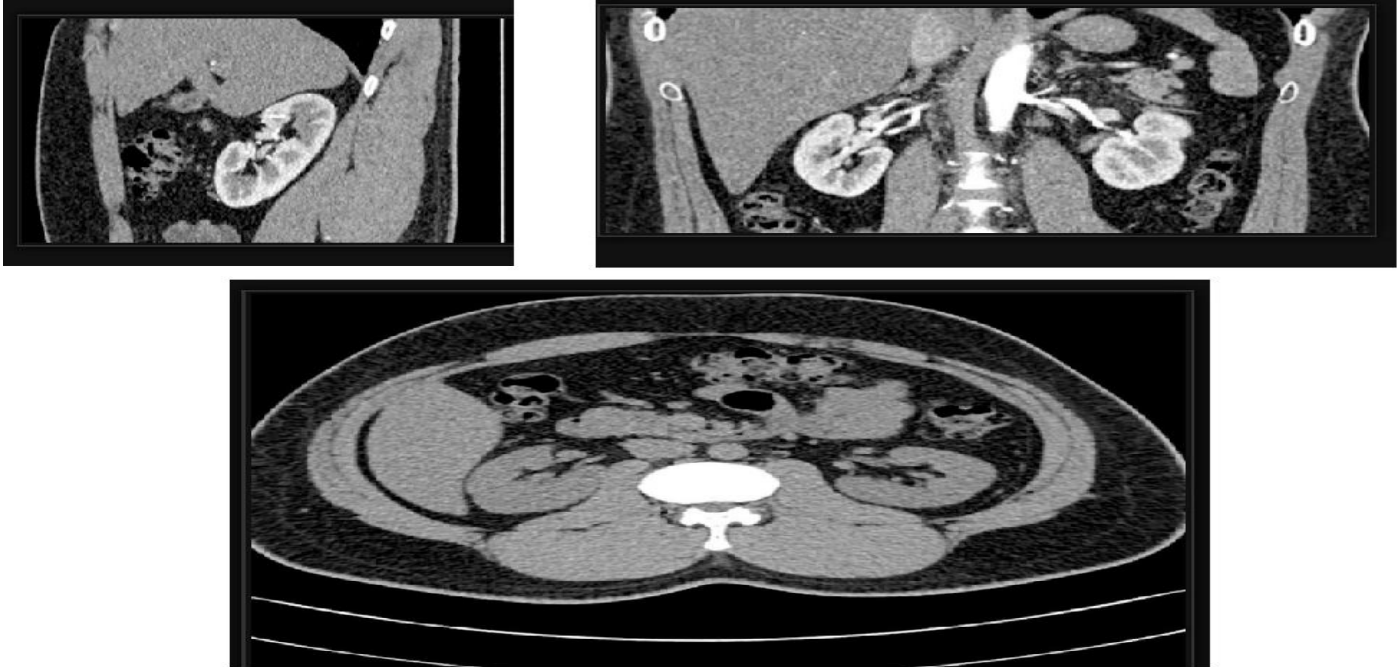


Figura 9 Anatomical planes

Sagittal

Coronal

2.4. Anatomy of the kidneys

are paired retroperitoneal organs that lie at the level of the T12 to L3 vertebral bodies.

The kidneys are located on the posterior abdominal wall, with one on either side of the vertebral column, in the perirenal space. The long axis of the kidney is parallel to the lateral border of the psaos muscle and lies on the quadratus lumborum muscle. In addition, the kidneys lie at an oblique angle, that is the superior renal pole is more medial and posteriorly than the inferior pole. Due to the right lobe of the liver, the right kidney usually lies slightly lower than the left kidney.

In adults, the normal kidney is 10-14 cm long in males and 9-13 cm long in females, 3-5 cm wide, 3 cm in antero-posterior thickness and weighs 150-260 g. The left kidney is usually slightly larger than the right.

The kidney is bean-shaped with a superior and an inferior pole, anterior and posterior surfaces, and lateral and medial borders. The midportion of the kidney is often called the midpole.

The kidney has a fibrous capsule, which is surrounded by perirenal fat. The kidney itself can be divided into renal parenchyma, consisting of renal cortex and medulla, and the renal sinus containing renal pelvis, calyces, renal vessels, nerves, lymphatics and perirenal fat.

The renal parenchyma has two layers: cortex and medulla. The renal cortex lies peripherally under the capsule while the renal medulla consists of 10-14 renal pyramids, which are separated from each other by an inward extension of the renal cortex called renal columns.

Urine is produced in the renal lobes, which consists of the renal pyramid with the associated overlying renal cortex and adjacent renal columns. Each renal lobe drains at a papilla into a minor calyx, four or five of these unite to form a major calyx. Each kidney normally has two or three major calyces, which unite to form the renal pelvis.

The renal hilum is the entry to the renal sinus and lies vertically at the anteromedial aspect of the kidney. It contains the renal vessels and nerves, fat and the renal pelvis, which typically emerges posterior to the renal vessels, with the renal vein being anterior to the renal artery.

Relations

- posterior
 - diaphragm (upper pole of the kidney)
 - parietal pleura through costal parts of diaphragm and lumbocostal trigone
 - parietal pleura that extends below 12th rib through lumbar part of diaphragm in costovertebral angle
 - 11th rib related to left kidney only (through costophrenic recess and diaphragm), 12th rib (directly)
 - lateral and medial lumbocostal arches (arcuate lines)
 - psoas major (medial margin of kidney and renal pelvis), quadratus lumborum
 - transversus abdominis (lateral margin of the kidney), subcostal nerve and iliohypogastric nerve
- anterior
 - right kidney
 - bare area of the liver (upper pole)
 - posterior portion of the right coronary ligament of liver (hepatorenal ligament)
 - parietal peritoneum
 - hepatorenal recess
 - right lobe of the liver
 - D2 duodenum (medial margin of the kidney)
 - right colic flexure (just above inferior pole)
 - left kidney
 - omental bursa/lesser sac (upper pole)
 - stomach
 - spleen (lateral margin)
 - tail of the pancreas (hilum)
 - loops of jejunum in the left infracolic compartment (lower pole)

- left colic flexure and descending colon (lateral to lower pole)
- superior
- adrenal glands

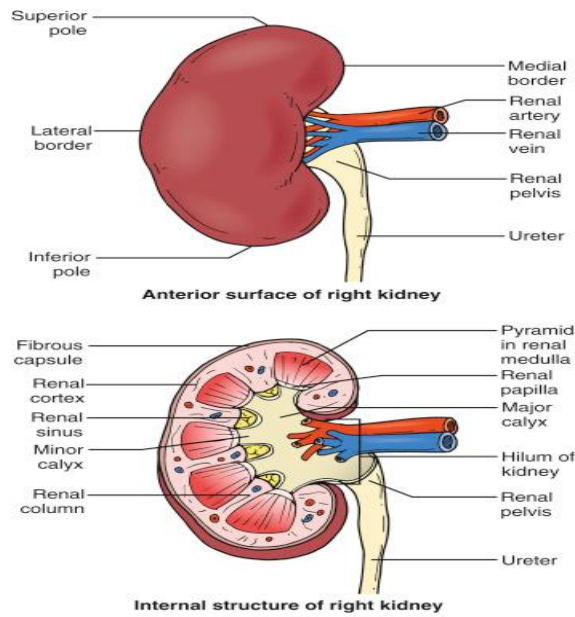


Figura 10 Anatomy of the urinary system. Cross-sectional anatomy of the kidney.

-Anatomical location of measurements of the renal vasculature. The segmental lines are as follows: (a and b) upper pole of the kidney that demonstrates the renal cortex, medulla and renal pyramids as well as the minor calyx and interlobular arteries; (c and d) renal cortex, medulla, renal pyramids, interlobular and main segmental renal arteries; and (e and f) inferior pole of the kidney that shows the renal cortex, medulla and renal pyramids as well as the minor calyx and interlobular arteries.

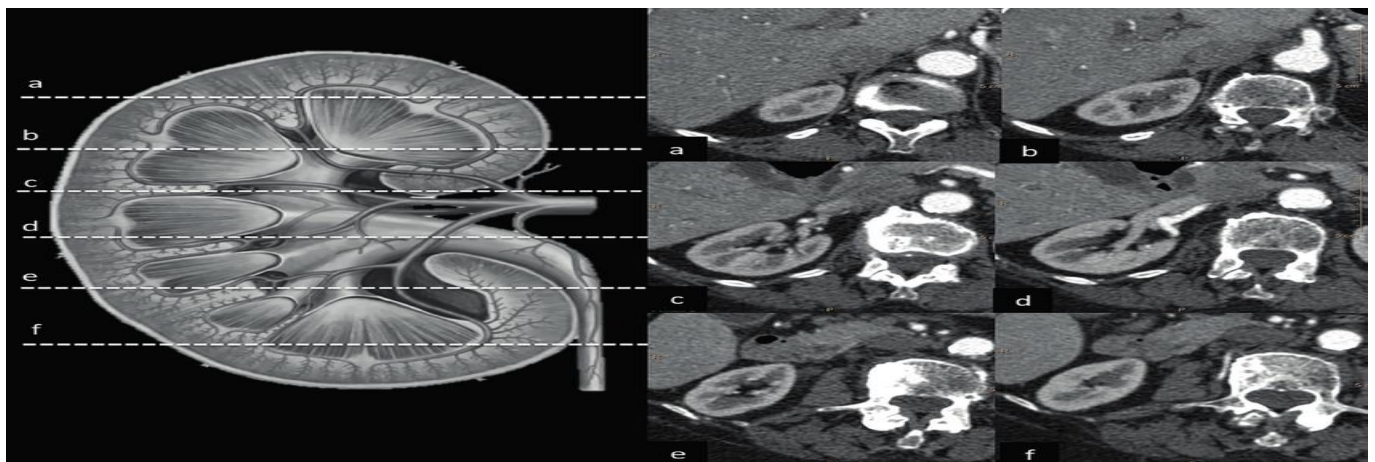
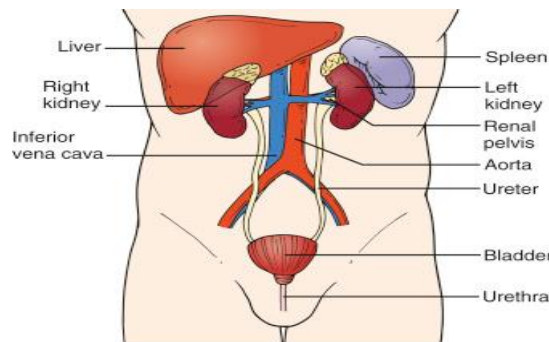


Figura 11 Kidney in (cT-scan)



Figura 12 Kidney in (cT-scan)

2.5. Clinical Examples

The CT-Scan findings in some typical examples of renal pathology are demonstrated.

2.6. Renal mass:

is an abnormal growth in the kidney. The majority of renal masses are benign; however, a significant number of them require further intervention. The retroperitoneum's anatomy, signs, symptoms, or physical examination are insufficient for detecting renal masses. Imaging modalities such as CT are used to diagnose such masses.

Renal masses are classified into either solid or cystic. This review will focus on the solid tumor with minimal discussion on the cystic type. One of the main concerns for a solid renal mass is carcinoma. There were about 74,000 new cases in 2019; of these, it is expected that 15,000 patients will die from cancer.

The five-year survival rate increases with early diagnosis. The survival rate for stage 1 and 2 renal cell carcinoma (RCC) is above 90% versus below 15% for certain types of stage 3 or metastatic disease.[1] Therefore, it is essential to diagnose and evaluate new renal masses in a timely manner to improve our patients' quality of life and prognosis. Arguably, the most critical indication of malignancy is the size of a tumor. Renal mass is commonly divided into two size categories; less than 4cm and more than 4cm. Because of the advancement of imaging tests such as CT, MRI, and ultrasound, more

A 66-year-old Man With Bilateral Renal Masses

masses are detected incidentally during other workups. A cross-sectional study performed in 2011 showed that renal masses are found incidentally in 14% of patients who underwent CT colonography.

Since renal mass is a diverse subject with many nuances in both treatment and management, this review will explore renal mass, emphasizing small renal masses because of clinical practice relevance. We will examine the etiologies, diagnosis, and management of renal mass.

2.7. Renal cell carcinoma

is the most common primary tumor of the kidney, with more than 30,000 new cases diagnosed in the United States each year. With the widespread use of cross-sectional imaging, many tumors are detected incidentally. Single- and multidetector computed tomography (CT) have helped refine the diagnostic work-

up of renal masses by allowing image acquisition in various phases of renal enhancement after intravenous administration of a single bolus of contrast material. The scanning protocol should include unenhanced CT followed by imaging during the corticomedullary and nephrographic phases of enhancement. The nephrographic phase is the most sensitive for tumoral detection, while the corticomedullary phase is essential for imaging the renal veins for possible tumoral extension and the parenchymal organs for potential metastases. Knowledge of the tumoral stage at the time of diagnosis is essential for prognosis and surgical planning. The accuracy of CT for staging has been reported to reach 91%, with most staging errors related to the diagnosis of perinephric extension of tumor. Three-dimensional CT provides the urologist with an interactive road map of the relationships among the tumor, the major vessels, and the collecting system. This information is particularly critical if the tumor extends into the inferior vena cava and if nephron-sparing surgery is being planned.

Renal cell carcinoma is the most common malignancy of the kidney and accounts for 2% of all cancers. It is estimated that 31,200 new cases were diagnosed during 2000 in the United States, and 11,900 of them will lead to death from the disease (1). To this day, complete surgical resection remains the only curative treatment for renal cell carcinoma.

The past 2 decades have witnessed significant changes in the manifestation, diagnosis, and management of renal cell carcinoma. With the widespread use of cross-sectional imaging, as many as one-half of such carcinomas are discovered incidentally and many are early-stage lesions. Paralleling this clinical stage migration is a growing trend for more limited surgical resection, such as adrenal-sparing radical nephrectomy, laparoscopic nephrectomy, or nephron-sparing partial nephrectomy (2). The challenges of renal tumoral imaging include not only reliable differentiation between benign and malignant lesions but also accurate delineation of the extent of the disease to ensure optimal treatment planning. Spiral computed tomography (CT) has significantly improved imaging of renal masses by decreasing volume averaging artifacts and respiratory misregistration artifacts and allowing image acquisition during optimal contrast enhancement. Further advances, particularly optimization of volume data sets, are anticipated with multidetector spiral CT, which provides better resolution than and data acquisition speeds at least four times greater than those of single-detector spiral CT. The objectives of this article are (a) to review and understand the protocols of single-detector and multidetector spiral CT for imaging renal cell carcinoma, (b) to present CT findings for staging of renal cell carcinoma, and (c) to discuss the value of three-dimensional CT in surgical planning and problem solving for patients with renal cell carcinoma.

2.8. Angiomylioma

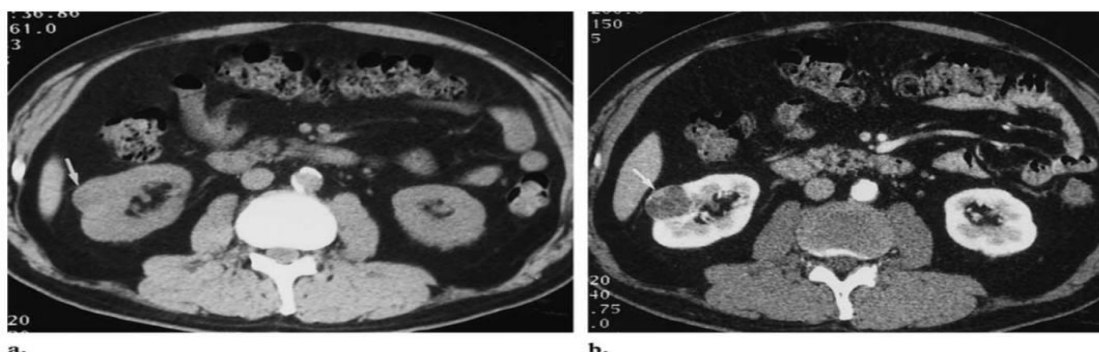


Figure 3 . Incidental renal cell carcinoma at unenhanced CT and at the corticomedullary and nephrographic phases of enhanced CT. (a) Unenhanced CT scan shows a 2.5-cm-diameter soft-tissue mass deforming the contour of the right kidney (arrow). (b) Contrast-enhanced CT scan obtained during the corticomedullary phase shows that the mass is hypodense compared with the renal cortex and has peripheral enhancement (arrow). The cortex is brightly enhanced, whereas the medulla is relatively unenhanced.

In this study we came across two cases of renal angiomyolipoma. Both the patients were teenage females (average age 18.5 years). In one case, the disease was unilateral while in the second there was bilateral involvement of the kidneys. One of the patients presented with classical Vogt's triad of tuberous sclerosis and showed bilateral small

Multiple renal angiomyolipomas. In addition to renal findings, CT also showed presence of hamartomas in liver which were identified by the characteristic presence of fat inside these lesions. CT scan of brain also showed multiple periventricular calcific densities typical of tuberous sclerosis lesions in the brain. Fundoscopy of the eyes showed characteristic potato tumors of retinal angiomas. X-ray hands and pelvis showed typical sclerotic lesions of tuberous sclerosis in the bones. Renal angiomyolipoma has to be differentiated from renal lipoma, retroperitoneal liposarcoma and renal cell carcinoma at CT. Presence of fat in the renal tumor is a sure indicator of renal angiomyolipoma; however, presence of solid density component causes diagnostic difficulties with renal cell carcinoma.

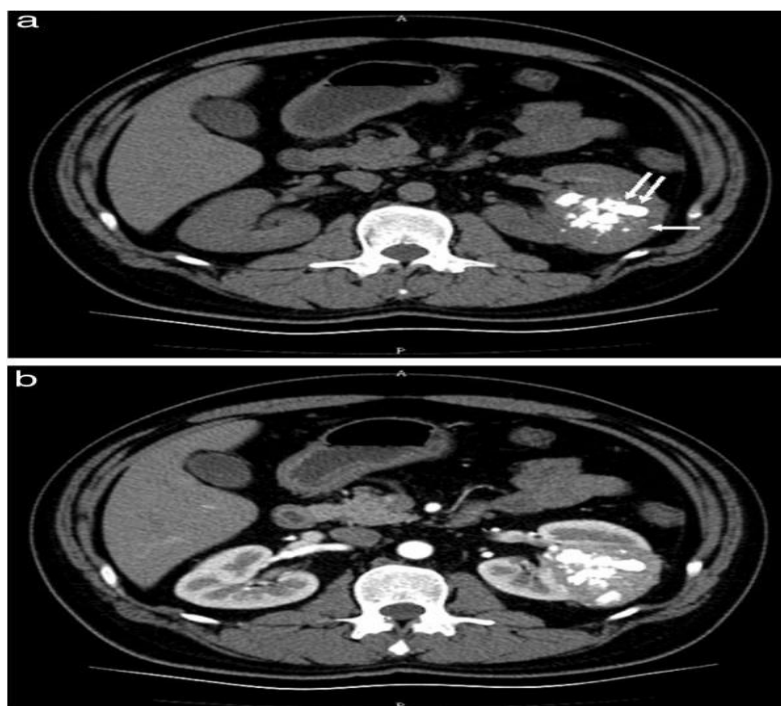


Figura 4 Angiomyolipoma

CT scan of the angiomyolipoma (AML) of the left kidney. (a) Noncontrast scan showing a solid tumor (arrow) with multiple calcifications (double arrow). (b) Contrast CT imaging showed contrast enhancement.

2.9. Renal Lymphomas

Primary renal lymphomas are rare as kidneys normally do not contain lymphoid tissue. Secondary involvement occurs due to disseminated disease or direct contiguous extension of retroperitoneal disease.

In this study we came across two cases of renal lymphoma constituting (5%) of all the renal tumors of this study. Non Hodgkin's lymphoma is commoner than Hodgkin's lymphoma, but the disease pattern remains same in both the conditions. In this study both the cases were proved to be non-Hodgkin's lymphoma at histopathology. Singer et al stated that CT findings of renal lymphoma are non specific and can be seen in other conditions also.⁷ Our study also revealed similar features.

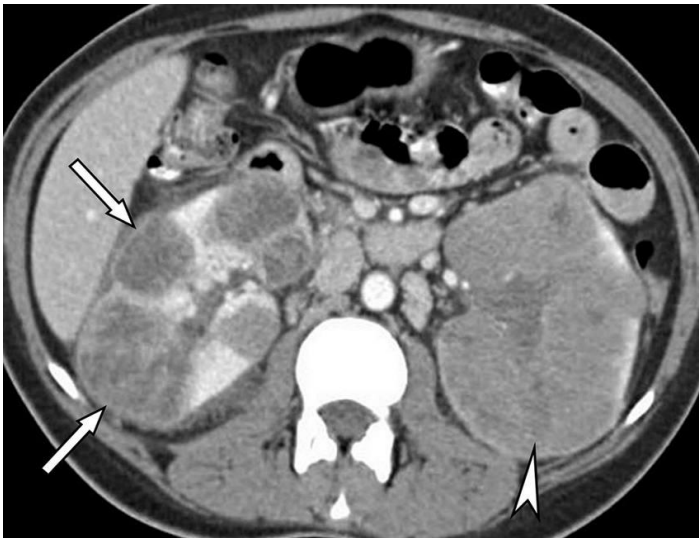


Figura 5 Renal Lymphomas

A 32-year-old Femal with biopsy-proven renal lymphoma. Axial contrast-enhanced CT shows multiple renal masses (arrows) in the right kidney and diffuse involvement of the left kidney (arrowhead). In our experience of CT and MRI of 35 cases of renal lymphoma, a mixed pattern was seen in 14 patients.

This chapter includes description indications, contraindications and patient preparation. In addition, basic protocols and planning used in this work.

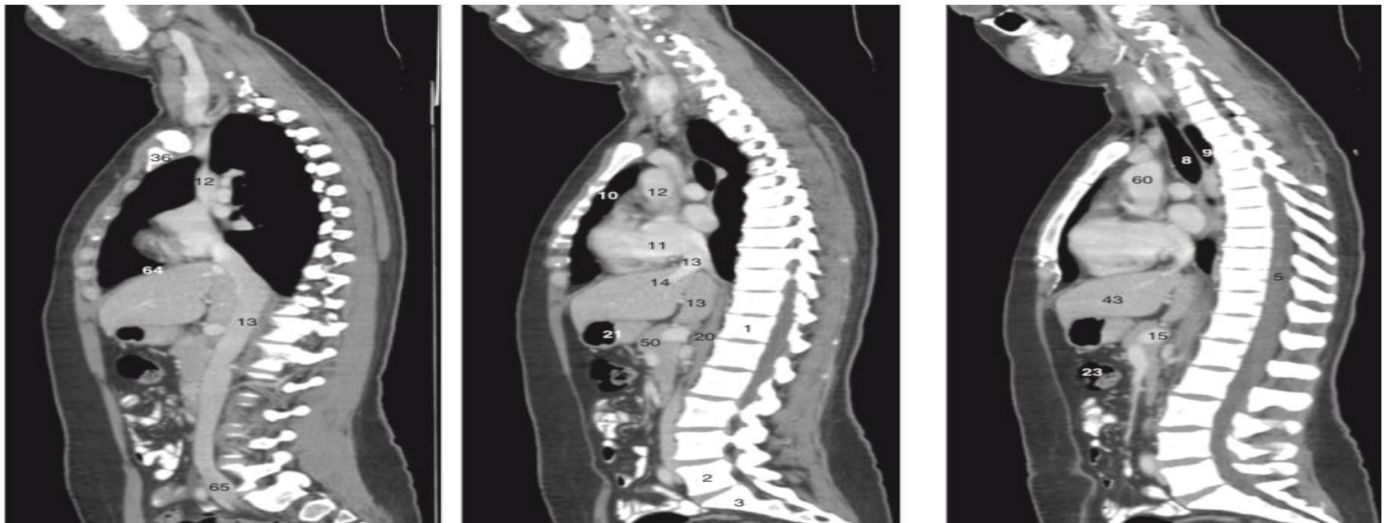


Figure 16 basic protocols and planning used

3.2. CT Sagittal Anatomy of Abdomen

a)–(h) abdomen and pelvis in a female, sequential sagittal CT images, from right to left.

1. Body of T12 vertebra
2. Body of L5 vertebra
3. Sacrum
4. Coccyx
5. Spinal cord
6. Cauda equina
7. Left renal vein
8. Trachea
9. Oesophagus

10. Right lung
11. Right atrium
12. Superior vena cava
13. Inferior vena cava
14. Hepatic vein
15. Splenic vein
16. Superior mesenteric vein 17. Superior mesenteric artery 18. Coeliac axis
19. Aorta
20. Right crus of diaphragm 21. Antrum of stomach
22. Descending colon
23. Transverse colon
24. Sigmoid colon
25. Rectum
26. Pubic body
27. Urinary bladder
28. Cervix
29. Vagina
30. Uterus (retroverted)
31. Gluteus maximus muscle 32. Iliac bone
33. Head of femur
34. Ischium
35. Body of sternum

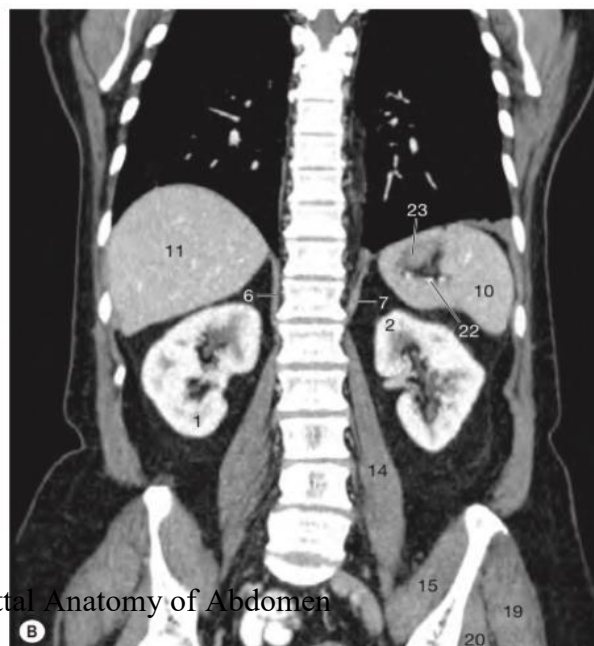


Figure 17 CT Sagittal Anatomy of Abdomen

3.3. CT coronal Anatomy of abdomen

Figure 5.46 • (A, B) Coronal reformatted CT of the abdomen showing kidneys and their relations

1. Right kidney (lower pole)
2. Left kidney (upper pole)
3. Renal pelvis
4. Left adrenal
5. Right adrenal
6. Crus right hemidiaphragm
7. Crus left hemidiaphragm
8. Aorta
9. IVC
10. Spleen
11. Liver
12. Tail of pancreas
13. Splenic flexure
14. Psoas muscle
15. Iliacus muscle
16. Transversus abdominis muscle
17. Internal oblique muscle
18. External oblique muscle
19. Gluteus maximus muscle
20. Gluteus medius muscle
21. Left hemidiaphragm
22. Hilum of spleen
23. Fundus of stomach

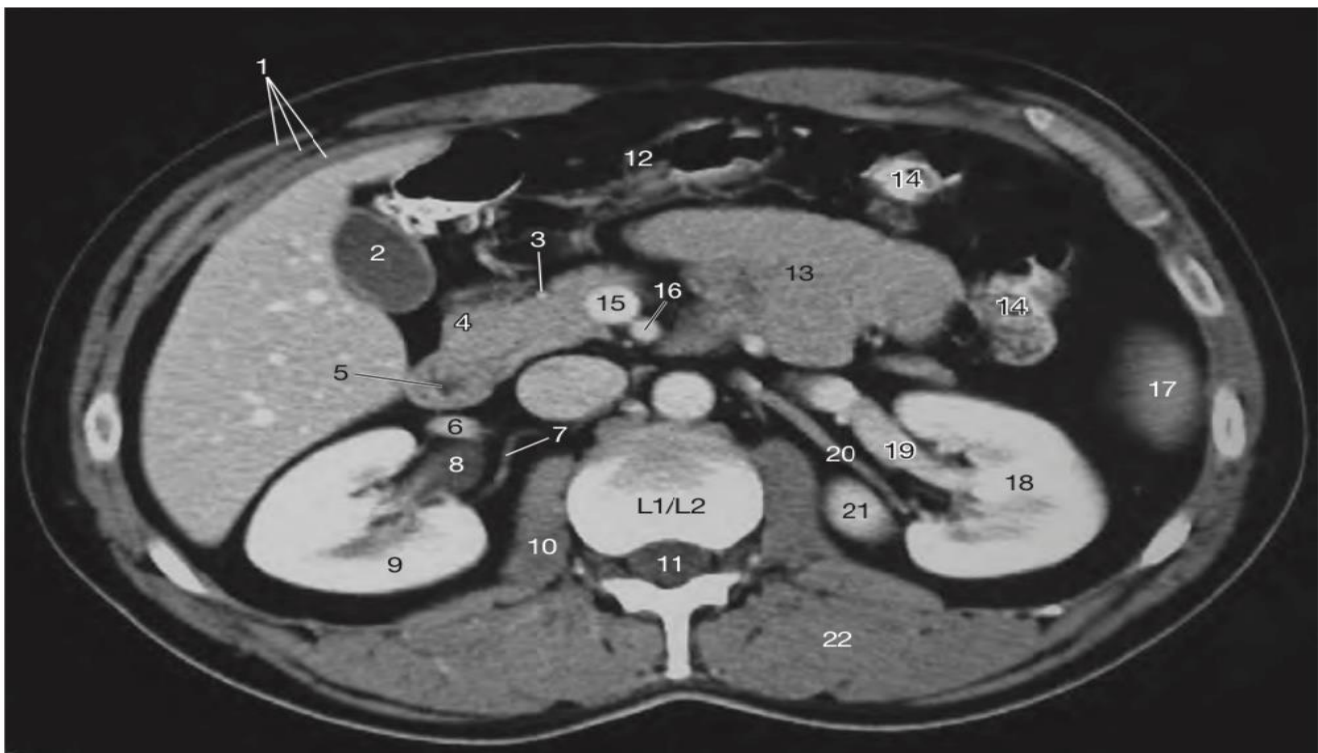


Figura 18 Axial CT of abdomen

3.4.CT Axial Anatomy of abdomen

1. Three layers of anterior abdominal wall
2. Gallbladder
3. Gastroduodenal artery
4. Head of pancreas
5. Duodenum
6. Renal vein
7. Branch of right renal artery
8. Ureter
9. Right kidney
10. Psoas muscle
11. Thecal sac in spinal canal
12. Transverse colon
13. Small bowel loops
14. Splenic flexure
15. Superior mesenteric vein
16. Superior mesenteric artery
17. Inferior pole of spleen
18. Left kidney at hilum
19. Left renal vein
20. Left renal artery
21. Renal lobulation
22. Erector spinae muscle

3.5. Indications for Abdomen CT scan

Indications for CT scanning include nephrolithiasis, kidney masses, traumatic injury to the kidney, staging renal tumors, polycystic kidney disease, and pyelonephritis. The primary limitation of CT scanning is the risk of radiation and administration of contrast. Acute undiagnosed abdominopelvic pain without a clear etiology, and accompanied by symptoms such as nausea, vomiting, diarrhea and/or issues with passing urine, is the primary indication for a CT KUB:

1. Renal colic/renal stone disease
2. Renal tumors
3. Renal/perirenal collection
4. Loin mass
5. Staging and follow-up of renal, collecting system or prostatic cancer.
6. Investigation of renal tract obstruction
7. CT angiography may be used to assess renal vessels for suspected renal artery stenosis or arteriovenous fistula or malformation.

3.6. Contraindications

Patients with reduced renal function are at risk of developing contrast-induced nephrotoxicity (CIN) following a contrast-enhanced computed tomography (CT) examination with an iodinated contrast agent 1 and at risk of developing nephrogenic systemic fibrosis (NSF) after a contrast-enhanced.

3.7. Patient preparation

CT scans may be performed on an outpatient basis or as part of your stay in a hospital. Procedures may vary depending on your condition and your physician's practices.

3.8. Generally, a CT scan follows this process:

1. You may be asked to change into a patient gown. If so, a gown will be provided for you. A locked will be provided to secure all personal belongings. Please remove all piercings and leave all jewelry and valuables at home.
2. If you are to have a procedure done with contrast, an intravenous (IV) line will be started in the hand or arm for injection of the contrast media. For oral contrast, you will be given a liquid contrast preparation to swallow. In some situations, the contrast may be given rectally.
3. You will lie on a scan table that slides into a large, circular opening of the scanning machine. Pillows and straps may be used to prevent movement during the procedure.
4. The technologist will be in another room where the scanner controls are located. However, you will be in constant sight of the technologist through a window. Speakers inside the scanner will enable the technologist to communicate with and hear you. You may have a call button so that you can let the technologist know if you have any problems during the procedure. The technologist will be watching you at all times and will be in constant communication.
5. As the scanner begins to rotate around you, X-rays will pass through the body for short amounts of time. You will hear clicking sounds, which are normal.
6. The X-rays absorbed by the body's tissues will be detected by the scanner and transmitted to the computer. The computer will transform the information into an image to be interpreted by the radiologist.
7. It will be important that you remain very still during the procedure. You may be asked to hold your breath at various times during the procedure.
8. If contrast media is used for your procedure, you may feel some effects when the media is injected into the IV line. These effects include a flushing sensation, a salty or metallic taste in the mouth, a brief headache, or nausea and/or vomiting. These effects usually last for a few moments.
9. You should notify the technologist if you feel any breathing difficulties, sweating, numbness or heart palpitations.
10. When the procedure has been completed, you will be removed from the scanner.
11. If an IV line was inserted for contrast administration, the line will be removed.



Figura 6 Generally, a CT scan follows this process

3.9. Positioning

The technologist begins by positioning you on the CT exam table, usually lying flat on your back. They may use straps and pillows to help you maintain the correct position and remain still during the exam. Many scanners are fast enough to scan children without sedation usually lying flat on your back or less commonly, on your side or on your stomach.

3.10. Basic protocols and planning

- non-contrast scan is best to determine the HU of homogenous renal mass or masses containing macroscopic fat ¹
- corticomedullary phase is best to delineate subcategories of renal cell carcinomas further
- nephrogenic phase is best for optimal enhancement of the renal parenchyma, including the renal medulla, and will demonstrate enhancing components of a mass
- excretory phase will demonstrate enhancement of calyces, renal pelvis and ureters. Many institutions will perform this around 5 minutes to demonstrate opacification of the ureters

Technique (4 phase)

- patient position
 - supine with their arms above their head
- scout
 - diaphragm to the lesser trochanter

Non-contrast scan

- scan extent
 - mid-diaphragm to the iliac crest (covering kidneys)
- scan direction
 - craniocaudal
- scan delay
 - none
- respiration phase
 - inspiration, breath-hold

Corticomedullary phase

- scan extent
 - mid-diaphragm to the iliac crest (covering kidneys)
- scan direction
 - craniocaudal
- contrast injection considerations (bolus tracking)
 - monitoring slice (region of interest)
 - level of the diaphragmatic hiatus or first lumbar vertebra at the aorta

- threshold
 - 150 HU
- volume
 - 100 mL of non-ionic contrast at 3 to 5 mL/s (a higher flow rate will equal greater enhancement)
- scan delay²
 - corticomedullary
 - 20-30 seconds post bolus trigger (30-40 s after injection)
- respiration phase
 - inspiration, breath-hold

Nephrogenic phase

- scan extent
 - mid-diaphragm to lesser trochanter (covering entire renal system)
- scan direction
 - craniocaudal
- contrast injection considerations
- scan delay
 - nephrographic phase
 - 100 seconds post-injection
- respiration phase
 - inspiration, breath-hold

Excretory phase

- scan extent
 - mid-diaphragm to lesser trochanter (covering entire renal system)
- scan direction
 - craniocaudal
- contrast injection considerations
- scan delay
 - excretory phase
 - 5-10 minutes post-injection
- respiration phase
 - inspiration, breath-hold



Figura 20 Basic protocols and planning

3.11. Practical points

- pseudoenhancement, an artifact encountered where the calculated density of a lesion is inaccurately increased, is a problem often noted in renal mass scans, dual-energy CT via virtual monoenergetic images at a KeV range of 80 KeV to 90 KeV can minimize beam hardening and partial voluming and overcome this issue

Results and Discussion

The results of cases of the Abdomen (KUB) region display in this chapter and has been procedures by CT-scan(Siemens) in Hilla General Teaching Hospital.

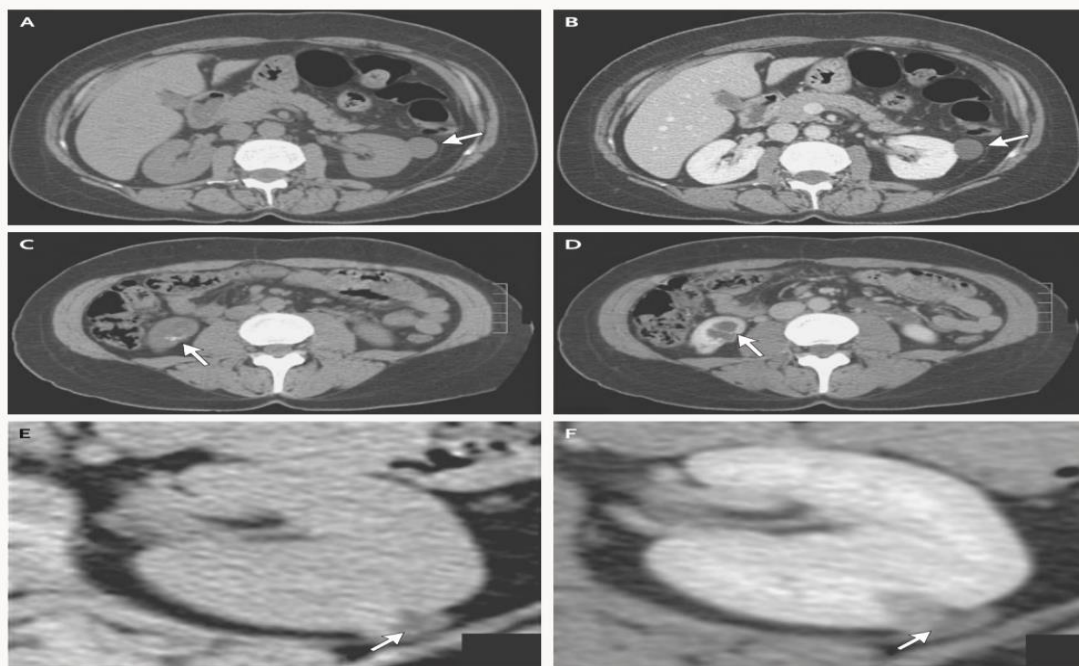


Figura 21 Cases of Abdomen CT

4.2. Cases of Abdomen CT

4.2.1 case one

4.2.2 Finding of Case One

Benign Renal Masses. Unenhanced (Panel A) and enhanced (Panel B) CT scans show no enhancement in a simple cyst (arrows; Bosniak class I) with the density of water and imperceptible walls. An unenhanced CT scan of a minimally complex cyst (Bosniak class IIF) shows discontinuous, slightly thick calcification (Panel C, arrow). An enhanced CT scan of the same cyst shows minimally thickened internal septation (Panel D, arrow), with perceptible enhancement but no enhancing mural nodules.

3rd Bosniak classification categorizes cystic masses on the basis of their radiologic characteristics. Class I lesions are benign, nonenhancing simple cysts with thin walls and without any septa, calcifications, or solid components. Class II lesions are benign cysts with a few hairline-thin septa; perceived enhancement, fine calcification, or a short segment of slightly thickened calcification may be present. Uniformly high-attenuation, well-marginated, nonenhancing lesions 3 cm in diameter or less (so-called high-density cysts) are included in this group. Cysts in this category do not require further evaluation. Class III cysts have multiple hairline-thin septa or minimal smooth thickening of the walls or septa that may contain thick and nodular calcification; these cysts do not have measurable contrast enhancement. Totally intrarenal, nonenhancing, high-attenuation renal lesions 3 cm in diameter or less are also included in this category. These lesions require follow-up studies to prove benignity. Class IV lesions are indeterminate cysts with thickened irregular or smooth walls or septa in which measurable enhancement is present; some are malignant. Class IV lesions are malignant; they have all the characteristics of class III cysts and also contain enhancing soft-tissue components adjacent to but independent of the wall or septum. Surgical removal is recommended. A small renal mass is shown in an unenhanced CT scan (Panel E, arrow) and in an enhanced scan (Panel F, arrow), with fat density diagnostic of angiomyolipoma.

4.2.3 Case Two

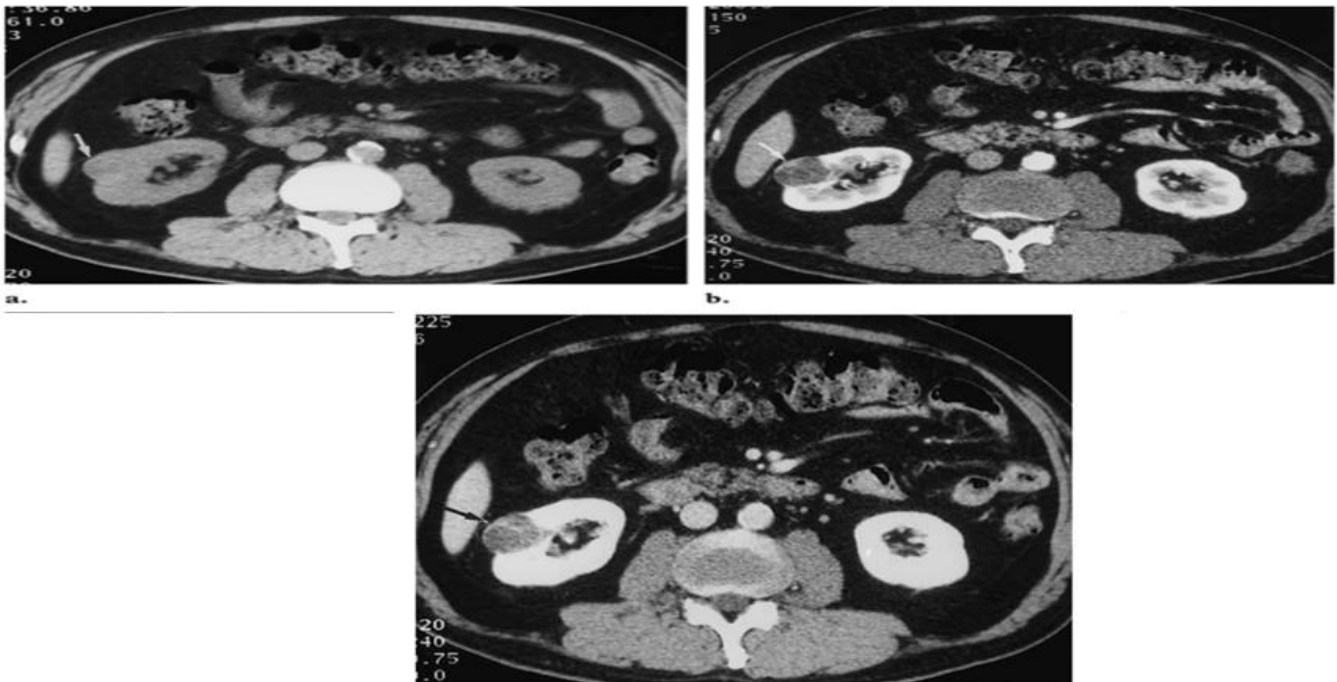


Figura 22 Case Two

4.2.4 Finding of Case Two

Incidental renal cell carcinoma at unenhanced CT and at the corticomedullary and nephrographic phases of enhanced CT. (a) Unenhanced CT scan shows a 2.5-cm-diameter soft-tissue mass deforming the contour of the right kidney (arrow). (b) Contrast-enhanced CT scan obtained during the corticomedullary phase shows that the mass is hypoattenuating compared with the renal cortex and has peripheral enhancement (arrow). The cortex is brightly enhanced, whereas the medulla is relatively unenhanced. (c) Contrast-enhanced CT scan obtained during the nephrographic phase shows the hypervascular mass is well demarcated from the homogeneously enhancing renal parenchyma (arrow). The patient underwent nephron-sparing nephrectomy. The pathologic stage was T1 NX.

4.2.5 Case Three

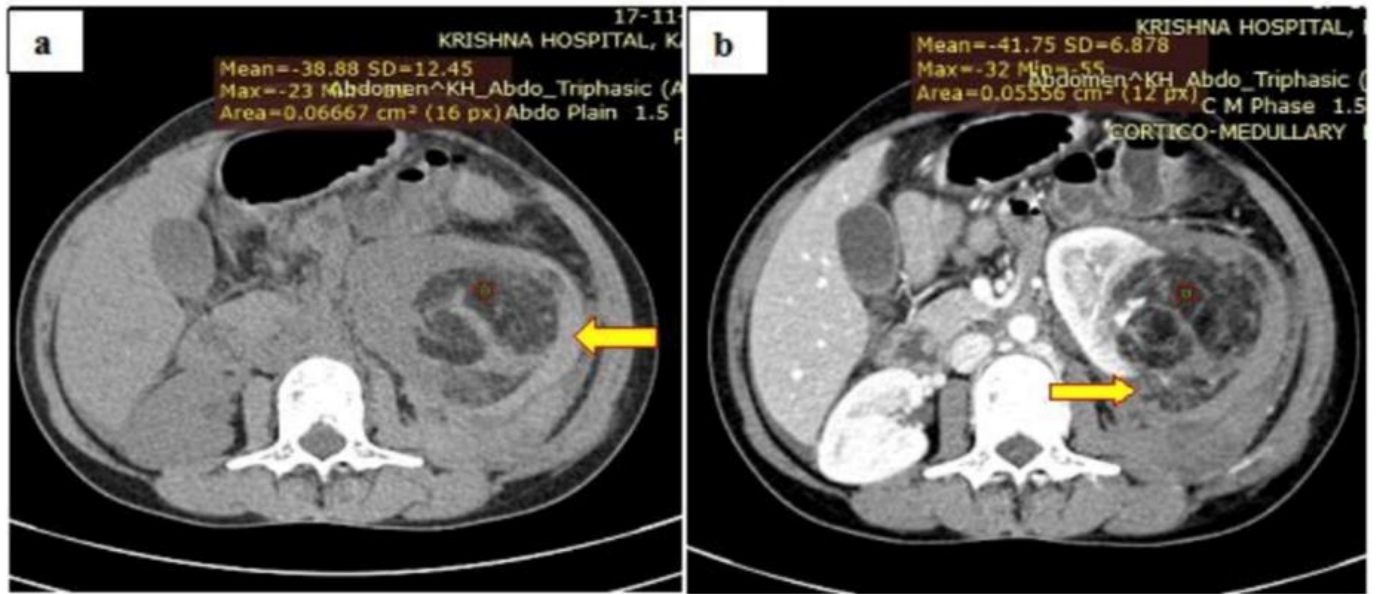


Figura 23 Case Three

4.2.6 Finding of Case Three

Case of Angiomyolipoma in 48 year old male patient (a) Axial Unenhanced CT demonstrates a well defined lesion arising from left kidney with fat attenuation and surrounding hyperdense collection. (b) Axial contrast image demonstrates heterogenous enhancement with non enhancing hyperdense collection.

4.2.7 Case Four

4.2.8 Finding of Case Four

case of renal metastases was seen in 65 year male who was known case of lung carcinoma on treatment for same. Lesion was hypoechoic on ultrasound and on CT lesion was showing peripheral enhancement with central necrotic non enhancing areas.

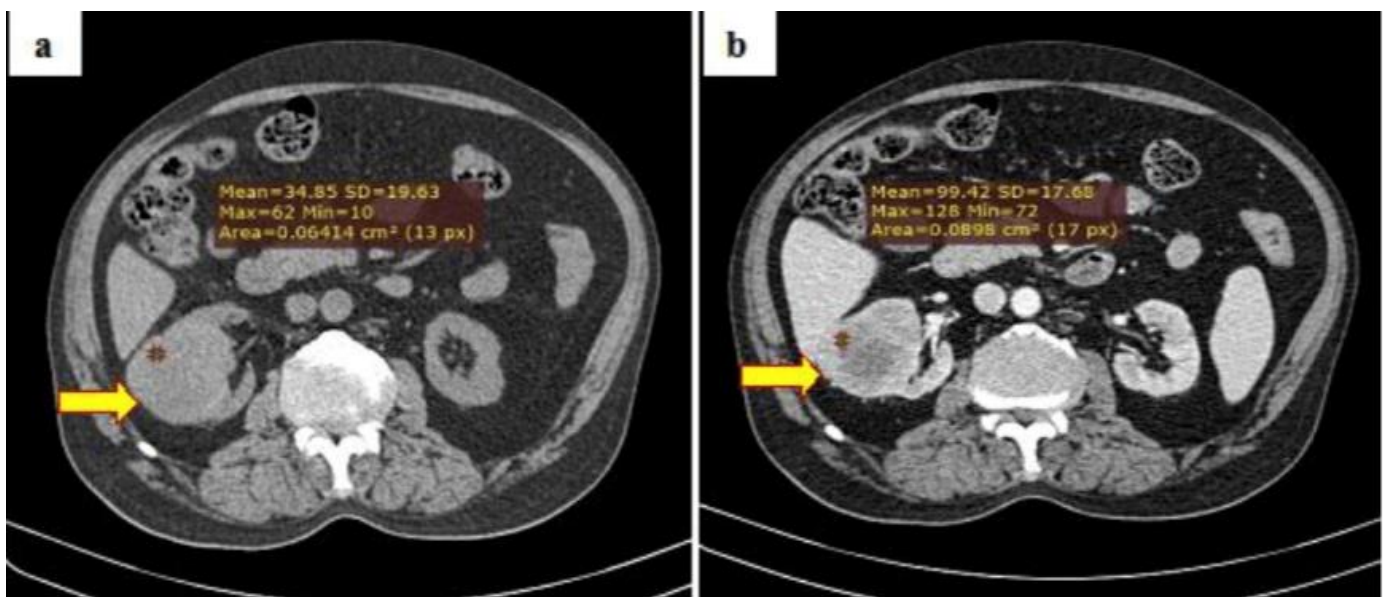


Figura 24 Case Four

4.2.9 Case Five

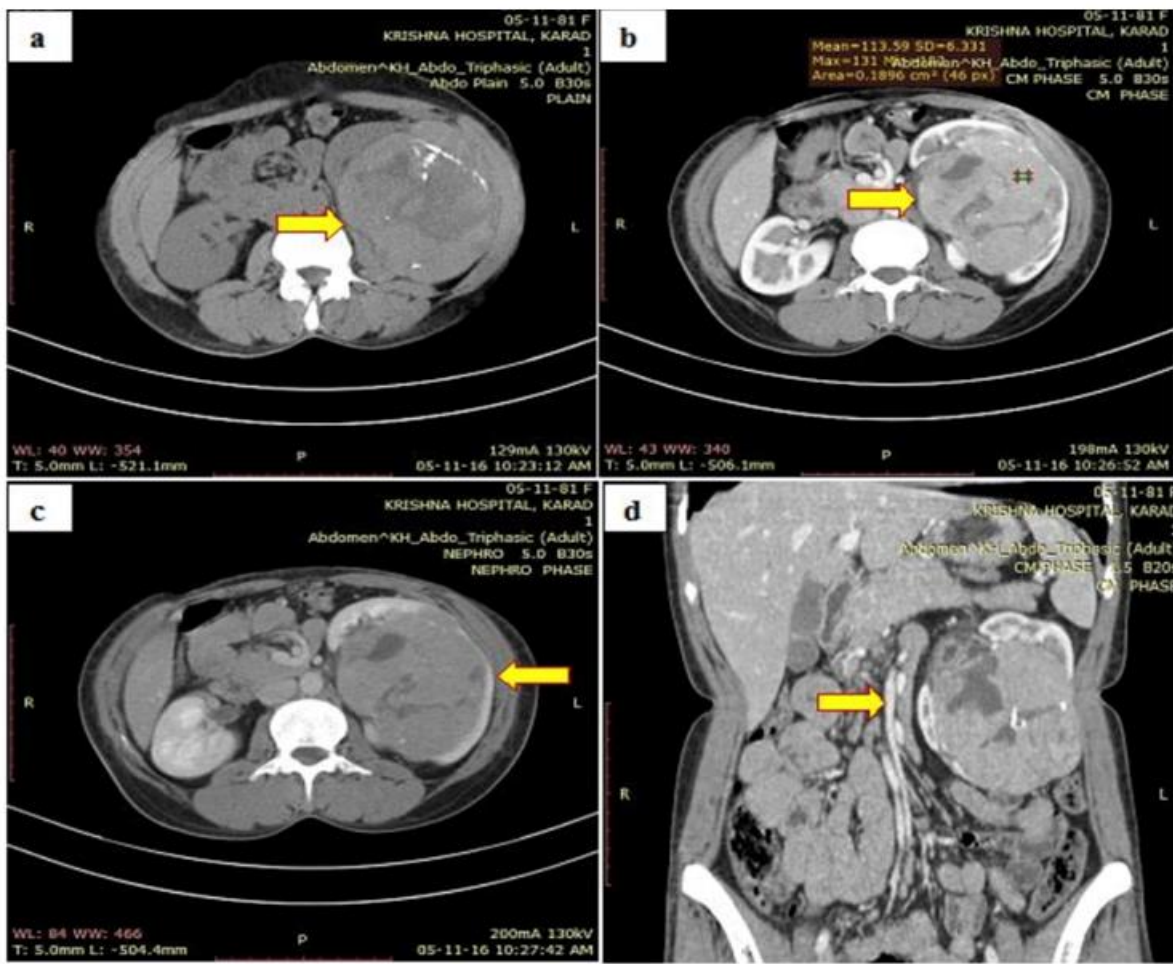


Figura 25 Case Five

4.2.10 Finding of Case Five

Case of renal cell carcinoma in middle aged male who presented with hematuria on CT a large lesion involving whole of the left kidney with maintained contour with abnormal renal axis and displacing adjacent structure. (a) Unenhanced CT shows heterogenous lesion with peripheral calcification. (b) and (c) CMP & NP showing heterogenous enhancement. (d) Coronal MPR image demonstrating entire involvement of left kidney.

Conclusion

Helical CT scan (CT-Scan) has become the main diagnosis of many kidney diseases (renal mass). where was The use of computed tomography in this research, as well as the assessment of image quality and diagnosis using the helical caliper, and to clarify common kidney diseases and how to diagnose them. This study also dealt with a brief description of CT scan, physics of CT-Scan imaging, CT-Scan technology and the protocols used. Several patients with different abdominal (kidney) symptoms were examined by CT-Scan type (Siemens) located in Hilla General Teaching Hospital. CT-Scan imaging provides technical flexibility and good diagnostic images, in addition to the fact that the diagnosis was perfect, which suits the patients' symptoms

Reference

1. Diagnosing non-hepatocellular carcinoma malignancies on CT/MRI and contrast enhanced ultrasound: the Liver Imaging Reporting and Data System approach
2. Kathryn J. Fowler et al., Hepatoma Research-OAE Publishing, 2020
3. Assessment of dual phase 18F-FDG PET/CT with contrast-enhanced CT for evaluation of primary renal neoplasms
4. ENTAO LIU et al., J Nucl Med, 2016
5. "Delayed Pial Vessels" in Multiphase CT Angiography Aid in the Detection of Arterial Occlusion in Anterior Circulation
6. R.-J. Singh et al., AJNR Am J Neuroradiol, 2018
7. CT and MRI of the liver for hepatocellular carcinoma
8. Cynthia Santillan, Hepatoma Research-OAE Publishing, 2020
9. Atypical Findings for a Typical Diagnosis: A Spectrum of Imaging Patterns for Oncocytoma
10. Margaret Houser et al., J Nucl Med, 2020
11. Zhipan's Account of the History of Buddhism in China: vol. 1, "Fozu tonghi," juan 34–38: From the Times of the Buddha to the Nanbeichao Era
12. Richard D. McBride, Sungkyun Journal of East Asian Studies, 2022.
13. "CT scan – Mayo Clinic". mayoclinic.org. Archived from the original on 15 October 2016. Retrieved 20 October 2016.
14. ^ "Patient Page". ARRT – The American Registry of Radiologic Technologists. Archived from the original on 9 November 2014.
15. ^ "Individual State Licensure Information". American Society of Radiologic Technologists. Archived from the original on 18 July 2013. Retrieved 19 July 2013.
16. ^ "The Nobel Prize in Physiology or Medicine 1979". NobelPrize.org. Retrieved 2019-08-10.
17. ^ Fishman, Elliot K.; Jeffrey, R. Brooke (1995). *Spiral CT: Principles, Techniques, and Clinical Applications*. Raven Press. ISBN 978-0-7817-0218-8.
18. ^ Hsieh, Jiang (2003). *Computed Tomography: Principles, Design, Artifacts, and Recent Advances*. SPIE Press. p. 265. ISBN 978-0-8194-4425-7.
19. ^ Stirrup, James (2020-01-02). *Cardiovascular Computed Tomography*. Oxford University Press. ISBN 978-0-19-880927-2.
20. ^ Talisetti, Anita; Jelnin, Vladimir; Ruiz, Carlos; John, Eunice; Benedetti, Enrico; Testa, Giuliano; Holterman, Ai-Xuan L.; Holterman, Mark J. (December 2004). "Electron beam CT scan is a valuable and safe imaging tool for the pediatric surgical patient". *Journal of Pediatric Surgery*. 39 (12): 1859–1862. doi:10.1016/j.jpedsurg.2004.08.024. ISSN 1531-5037. PMID 15616951.
21. ^ Retsky, Michael (31 July 2008). "Electron beam computed tomography: Challenges and opportunities". *Physics Procedia*. 1 (1): 149–154. Bibcode:2008PhPro...1..149R. doi:10.1016/j.phpro.2008.07.090.
22. ^ Carrascosa, Patricia M.; Cury, Ricardo C.; García, Mario J.; Leipsic, Jonathon A. (2015-10-03). *Dual-Energy CT in Cardiovascular Imaging*. Springer. ISBN 978-3-319-21227-2.
23. ^ Schmidt, Bernhard; Flohr, Thomas (2020-11-01). "Principles and applications of dual source CT". *Physica Medica*. 125 Years of X-Rays. 79: 36–46. doi:10.1016/j.ejmp.2020.10.014. ISSN 1120-1797.

24. ^ a b Schulsinger DA (2014). *Kidney Stone Disease: Say NO to Stones!*. Springer. p. 27. ISBN 9783319121055. Archived from the original on 8 September 2017.
25. ^ a b c d e f g h i j k l m n o p q r s "Kidney Stones in Adults". February 2013. Archived from the original on 11 May 2015. Retrieved 22 May 2015.
26. Becker KL (2001). *Principles and practice of endocrinology and metabolism* (3 ed.). Philadelphia, Pa. [u.a.]: Lippincott, Williams & Wilkins. p. 684. ISBN 978-0-7817-1750-2. Archived from the original on 8 September 2017.
27. ^ "Cystine stones". UpToDate. Archived from the original on 26 February 2014. Retrieved 20 February 2014.
28. ^ Bailey & Love's/25th/1296
29. ^ National Endocrine and Metabolic Diseases Information Service (2008). "Renal Tubular Acidosis (NIH Publication No. 09-4696)". *Kidney & Urologic Diseases: A-Z list of Topics and Titles*. Bethesda, Maryland: National Institute of Diabetes and Digestive and Kidney Diseases, National Institutes of Health, Public Health Service, US Department of Health and Human Services. Archived from the original on 28 July 2011. Retrieved 27 July 2011.
30. ^ a b c d De Mais D (2009). *ASCP Quick Compendium of Clinical Pathology* (2nd ed.). Chicago: ASCP Press.
31. ^ a b c d e Weiss M, Liapis H, Tomaszewski JE, Arend LJ (2007). "Chapter 22: Pyelonephritis and Other Infections, Reflux Nephropathy, Hydronephrosis, and Nephrolithiasis". In Jennette JC, Olson JL, Schwartz MM, Silva FG (eds.). *Heptinstall's Pathology of the Kidney*. Vol. 2 (6th ed.). Philadelphia: Lippincott Williams & Wilkins. pp. 991–1082. ISBN 978-0-7817-4750-9. Archived from the original on 20 March 2021. Retrieved 6 November 2020.
32. ^ Halabe A, Sperling O (1994). "Uric acid nephrolithiasis". *Mineral and Electrolyte Metabolism*. 20 (6): 424–31. PMID 7783706.
33. Smith RC, Varanelli M (July 2000). "Diagnosis and management of acute ureterolithiasis: CT is truth". *AJR. American Journal of Roentgenology*. 175 (1): 3–6. doi:10.2214/ajr.175.1.1750003. PMID 10882237.
34. ^ Bushinsky D, Coe FL, Moe OW (2007). "Ch. 37: Nephrolithiasis". In Brenner BM (ed.). *Brenner and Rector's The Kidney*. Vol. 1 (8th ed.). Philadelphia: WB Saunders. pp. 1299–349. ISBN 978-1-4160-3105-5. Archived from the original on 8 October 2011.
35. ^ Smith RC, Levine J, Rosenfeld AT (September 1999). "Helical CT of urinary tract stones. Epidemiology, origin, pathophysiology, diagnosis, and management". *Radiologic Clinics of North America*. 37 (5): 911–52, v. doi:10.1016/S0033-8389(05)70138-X. PMID 10494278.
36. ^ American College of Emergency Physicians (27 October 2014). "Ten Things Physicians and Patients Should Question". *Choosing Wisely*. Archived from the original on 7 March 2014. Retrieved 14 January 2015.
37. ^ "American Urological Association | Choosing Wisely". www.choosingwisely.org. Archived from the original on 23 February 2017. Retrieved 28 May 2017.
38. ^ a b c Fang LS (2009). "Chapter 135: Approach to the Patient with Nephrolithiasis". In Goroll AH, Mulley AG (eds.). *Primary care medicine: office evaluation and management of the adult patient*

- (6th ed.). Philadelphia: Lippincott Williams & Wilkins. pp. 962–7. ISBN 978-0-7817-7513-7. Archived from the original on 21 March 2021. Retrieved 6 November 2020.
39. ^ a b Semins MJ, Matlaga BR (September 2013). "Management of urolithiasis in pregnancy". *International Journal of Women's Health*. 5: 599–604. doi:10.2147/ijwh.s51416. PMC 3792830. PMID 24109196.
 40. ^ Smith-Bindman R, Aubin C, Bailitz J, Bengiamin RN, Camargo CA, Corbo J, et al. (September 2014). "Ultrasonography versus computed tomography for suspected nephrolithiasis" (PDF). *The New England Journal of Medicine*. 371 (12): 1100–10. doi:10.1056/NEJMoa1404446. PMID 25229916. Archived (PDF) from the original on 14 March 2020. Retrieved 25 September 2019.
 41. ^ National Kidney and Urologic Diseases Information Clearinghouse (2007). "Kidney Stones in Adults (NIH Publication No. 08–2495)". *Kidney & Urologic Diseases: A-Z list of Topics and Titles*. Bethesda, Maryland: National Institute of Diabetes and Digestive and Kidney Diseases, National Institutes of Health, Public Health Service, US Department of Health and Human Services. Archived from the original on 26 July 2011. Retrieved 27 July 2011.
 42. ^ Becker KL (2001). *Principles and practice of endocrinology and metabolism* (3 ed.). Philadelphia, Pa. [u.a.]: Lippincott, Williams & Wilkins. p. 684. ISBN 978-0-7817-1750-2. Archived from the original on 8 September 2017.
 43. ^ "Cystine stones". *UpToDate*. Archived from the original on 26 February 2014. Retrieved 20 February 2014.